

WILEY

Online Proofing System

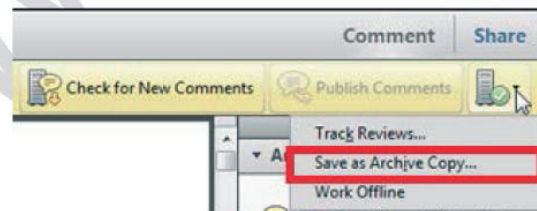
1. Corrections should be marked with the Adobe Annotation & Comment Tools below:



2. To save your proof corrections, click the 'Publish Comments' button. Publishing your comments saves the marked up version of your proof to a centralized location in Wiley's Online Proofing System. Corrections don't have to be marked in one sitting – you can publish corrections and log back in at a later time to add more.



3. When your proof review is complete we recommend you download a copy of your annotated proof for reference in any future correspondence concerning the article before publication. You can do this by clicking on the icon to the right of the 'Publish Comments' button and selecting 'Save as Archive Copy...'



4. When your proof review is complete and you are ready to send corrections to the publisher click the 'Complete Proof Review' button that appears above the proof in your web browser window. Do not click the 'Finalize/Complete Proof Review' button without replying to any author queries found on the last page of your proof. Incomplete proof reviews will cause a delay in publication. **Note: Once you click 'Finalize/Complete Proof Review' you will not be able to mark any further comments or corrections.**



Firefox, Chrome, Safari Users

If your PDF article proof opens in any PDF viewer other than Adobe Reader or Adobe Acrobat, you will not be able to mark corrections and query responses, nor save them. To mark and save corrections, please follow these [instructions to disable the built-in browser PDF viewers in Firefox, Chrome, and Safari](#) so the PDF article proof opens in Adobe within a Firefox or Chrome browser window.

Once you have Acrobat Reader open on your computer, click on the [Comment](#) tab at the right of the toolbar:



This will open up a panel down the right side of the document. The majority of tools you will use for annotating your proof will be in the [Annotations](#) section, pictured opposite. We've picked out some of these tools below:



1. Replace (Ins) Tool – for replacing text.



Strikes a line through text and opens up a text box where replacement text can be entered.

How to use it

- Highlight a word or sentence.
- Click on the [Replace \(Ins\)](#) icon in the Annotations section.
- Type the replacement text into the blue box that appears.

standard framework for the analysis of microeconomic policy. Nevertheless, it also led to the development of a number of strategic substitutes. The number of competitors in the industry is that the structure of the industry, which led to the main components of the industry level, are explained by the important works on entry by Shirasaka (M henceforth)¹ we open the 'black b



2. Strikethrough (Del) Tool – for deleting text.



Strikes a red line through text that is to be deleted.

How to use it

- Highlight a word or sentence.
- Click on the [Strikethrough \(Del\)](#) icon in the Annotations section.

there is no room for extra profits and mark-ups are zero and the number of firms (net) values are not determined by the Blanchard and Kiyotaki (1987), perfect competition in general equilibrium of aggregate demand and supply in a classical framework assuming monopoly. An exogenous number of firms

3. Add note to text Tool – for highlighting a section to be changed to bold or italic.



Highlights text in yellow and opens up a text box where comments can be entered.

How to use it

- Highlight the relevant section of text.
- Click on the [Add note to text](#) icon in the Annotations section.
- Type instruction on what should be changed regarding the text into the yellow box that appears.

dynamic responses of mark-ups consistent with the VAR evidence

sation by Mar... and... on... to a... on... stent also with the demand-



4. Add sticky note Tool – for making notes at specific points in the text.

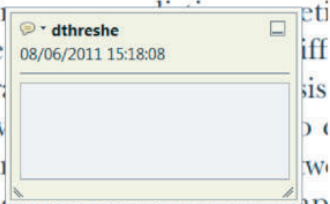


Marks a point in the proof where a comment needs to be highlighted.

How to use it

- Click on the [Add sticky note](#) icon in the Annotations section.
- Click at the point in the proof where the comment should be inserted.
- Type the comment into the yellow box that appears.

and supply shocks. Most of the... number of... standard fr... ical. Nev... ole of st... ber of competitors and the imp... is that the structure of the secto





5. Attach File Tool – for inserting large amounts of text or replacement figures.

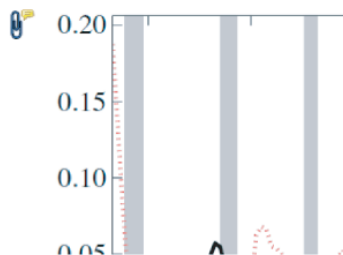


Inserts an icon linking to the attached file in the appropriate place in the text.

How to use it

- Click on the **Attach File** icon in the Annotations section.
- Click on the proof to where you'd like the attached file to be linked.
- Select the file to be attached from your computer or network.
- Select the colour and type of icon that will appear in the proof. Click OK.

END



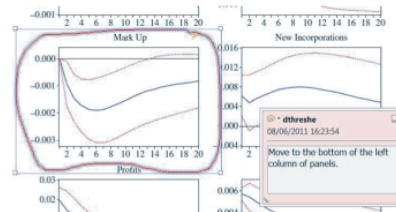
6. Drawing Markups Tools – for drawing shapes, lines and freeform annotations on proofs and commenting on these marks.

Allows shapes, lines and freeform annotations to be drawn on proofs and for comment to be made on these marks.



How to use it

- Click on one of the shapes in the Drawing Markups section.
- Click on the proof at the relevant point and draw the selected shape with the cursor.
- To add a comment to the drawn shape, move the cursor over the shape until an arrowhead appears.
- Double click on the shape and type any text in the red box that appears.





Novel thermal curing of cycloaliphatic resins by thiol–epoxy click process with several multifunctional thiols

Dailyñ Guzmán,^a Blai Mateu,^a Xavier Fernández-Francos,^b Xavier Ramis^b and Angels Serra^{a*}

Abstract

Novel thermosets were prepared by the base-catalysed reaction between a cycloaliphatic resin (ECC) and various thiol crosslinkers. 4-(*N,N*-Dimethylaminopyridine) (DMAP) was used as base catalyst for the thiol–epoxy reaction. A commercial tetrathiol (PETMP) and three different thiols synthesized by us, 6SH-SQ, 3SH-EU and 3SH-ISO, were tested. 6SH-SQ and 3SH-EU were prepared from vinyl or allyl compounds from renewable resources such as squalene and eugenol, respectively. Thiol 3SH-ISO was prepared starting from commercially available triallyl isocyanurate. A kinetic study of the mixtures was performed using differential scanning calorimetry. Stoichiometric ECC/thiol/DMAP formulations were cured at 120 °C for 1 h, at 150 °C for 1 h and post-cured for 30 min at 200 °C. The materials were characterized using Fourier transform infrared spectroscopy, thermogravimetric analysis and dynamic mechanical thermal analysis. The results revealed that the materials obtained from the synthesized thiols had higher thermal stability and glass transition temperatures than those obtained from the commercial PETMP. In addition, all the materials obtained exhibited very good transparency. This study proves the ability of multifunctional thiols to crosslink cycloaliphatic epoxy resins, leading to more flexible materials than those obtained by cationic homopolymerization of ECC or base-catalysed ECC–anhydride copolymerization.

© 2017 Society of Chemical Industry

Supporting information may be found in the online version of this article.

Keywords: cycloaliphatic epoxides; thiol–epoxy; click; thermosets; eugenol; squalene

INTRODUCTION

There is no doubt that click reactions are highly interesting tools in the organic chemistry synthetic world. The philosophy of click chemistry is based on generating new substances starting from small units, by highly controlled reactions, clean and energy saving processes without the formation of by-products or organic volatiles, emulating nature.^{1–3} The thiol–epoxy reaction is a good example among the great variety of click reactions.⁴ Its mechanism is based on the nucleophilic attack to a less substituted carbon on an epoxy ring by a thiolate anion.^{5,6}

In recent years, thiol–epoxy reactions have been applied in the curing of epoxy resins, specifically for diglycidyl ether of bisphenol A (DGEBA), obtaining materials with good thermal properties and high transparency.⁷ Although DGEBA resins are the most widely used for various applications, cycloaliphatic epoxy resins present some advantages that make them more applicable in the electrical and electronic industries. Among their most notable features, excellent weathering, inherently low viscosity, low dielectric loss and high electrical resistivity are of utmost importance for the fabrication of electronic devices. Because of their high resistance to yellowing by UV light absorption, they are also useful in applications like light-emitting diodes. Wang's group synthesized and characterized a great variety of cycloaliphatic epoxy resins with different structures for several special applications,^{8,9} among them for optical materials,¹⁰ electronics¹¹ or fire retardancy,¹²

but nowadays the most widely used in industrial applications is 3,4-epoxycyclohexyl-3',4'-epoxycyclohexanecarboxylate (ECC).

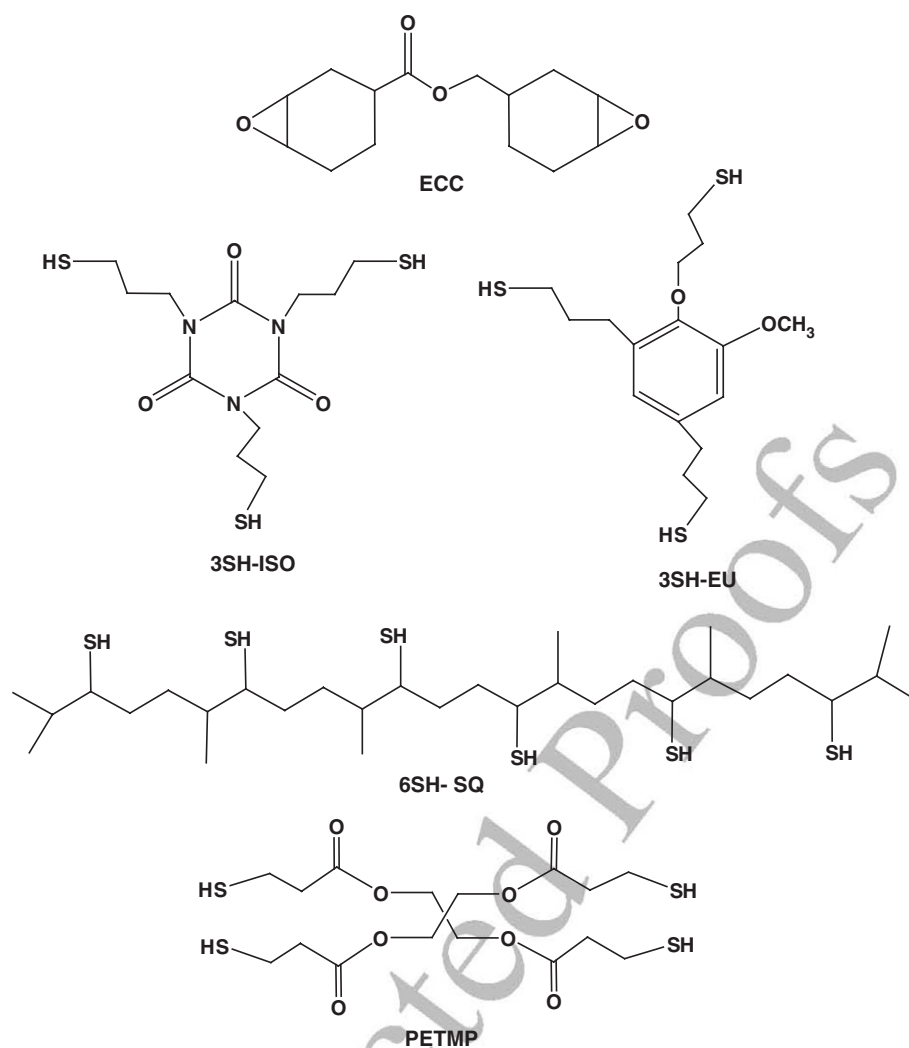
Cycloaliphatic epoxy resins are more reactive than DGEBA in the presence of cationic curing agents and therefore these resins are usually homopolymerized via cationic ring-opening in thermal or photoinitiated conditions.^{13,14} Cycloaliphatic epoxy resins are not reactive by nucleophilic attack of amines because of the high topological hindrance of the epoxy in the cycloaliphatic ring. However, they can be cured by anhydrides through a ring-opening copolymerization mechanism.^{15,16} Homopolymerized and anhydride-cured cycloaliphatic epoxy resins are usually brittle materials because of the compact and rigid nature of the network structure and the inherent rigidity of the network chains. Therefore, it is quite interesting to modify the network by curing with other stoichiometric hardeners or copolymerization with flexible comonomers, leading to more open and flexible

* Correspondence to: Angels Serra, Department of Analytical and Organic Chemistry, University Rovira i Virgili, C/ Marcel·lí Domingo s/n, 43007 Tarragona, Spain. E-mail: angels.serra@urv.cat

^a Department of Analytical and Organic Chemistry, University Rovira i Virgili, Spain

^b Thermodynamics Laboratory, ETSEIB University Politècnica de Catalunya, Spain





Scheme 1. Chemical structures of the epoxy resin and the thiols studied.

network structures and with higher versatility in mechanical and thermomechanical behaviour.¹⁷

The use of thiols as crosslinking agents in thiol–ene, thiol–epoxy or thiol–acrylate materials^{18,19} is a good strategy to obtain materials with a flexible network structure and lower crosslinking density than homopolymerized thermosets, with a subsequent increase in toughness or impact resistance. By selecting the structure and functionality of the thiol, glass transition temperature (T_g) and modulus of the cured materials can be adequately tailored.²⁰ The curing of ECC by thiol–epoxy click reactions has been little explored, the only report in the literature being the investigation of Sangermano *et al.*²¹ They prepared hybrid nanocomposites using a combination of thiol–epoxy and sol–gel processes. As starting formulations, they used various mixtures of commercial trithiol and a photolabile tertiary amine, ECC, tetraethoxysilane and 3-mercaptopropyltrimethoxysilane. They obtained organic/inorganic hybrid materials with a potential interest for optical applications. However, such systems are only adequate for thin layers, because of the limitations of photoirradiation technologies.

Thiols from renewable sources are very attractive because they are a good alternative for preparing thermosets from non-petroleum based-derivatives. Among natural products,

terpenes show a high functionality in a quite compact structure and therefore they are good candidates for thermosetting materials. Acosta Ortiz *et al.*²² reported the preparation of a hexathiol derivative of squalene prepared through a thiol–ene reaction preceded by hydrolysis. It has, in principle, a flexible aliphatic structure but, given its high functionality and the low molecular weight of each reactive unit, once the material is crosslinked, the presence of internal branching points and the short distance between crosslinking points would lead to rigid materials with high T_g . Following the same synthetic procedure, two new trithiols with rigid core were also synthesized. One of them is derived from eugenol, which is also a natural product, and the other is derived from commercially available triallyl isocyanurate (Scheme 1).

In this paper we describe the curing of a cycloaliphatic epoxy resin (ECC) with the three thiols synthesized and we also include the widely used and commercially available tetrafunctional thiol pentaerythritol tetrakis(3-mercaptopropionate) (PETMP), with a highly flexible structure. The kinetics of the curing process was analysed using calorimetry. The crosslinked materials obtained were characterized using thermogravimetry and thermomechanical analysis.



EXPERIMENTAL

Materials

ECC, eugenol (EU), squalene (SQ), triallyl isocyanurate (TAIC), PETMP, thioacetic acid (TAA), allyl bromide, 2,2-dimethoxy-2-phenylacetophenone (DMPA), 4-(*N,N*-dimethylamino)pyridine (DMAP), 1-methylimidazole (1-MI) and 2-methylimidazole (2-MI) were purchased from Sigma-Aldrich and were used without further purification. The latent amine precursor was LC-80 (encapsulated imidazole) and was obtained from AC Catalysts. Inorganic salts and bases were purchased from Scharlab. Methanol from Carlo Erba was used as received. *N,N*-Dimethylformamide (DMF) from VWR was dried using standard procedures.

Preparation of starting products

Synthesis of thiol from squalene (6SH-SQ)

The product was obtained following a two-step procedure previously reported.²²

Photochemical thiol-ene reaction (6STA-SQ). A mixture of 5 g (12.2 mmol) of SQ, 11.1 g (146 mmol) of TAA and 0.062 g (0.24 mmol) of DMPA was photoirradiated with a UV lamp at 356 nm for 30 min. The product was dissolved in CHCl₃ and extracted with a 10% NaOH solution and then washed with water and dried over anhydrous MgSO₄. The solvent was removed using a rotary evaporator. A clear viscous liquid was obtained in 87% yield. ¹H NMR (CDCl₃; δ , ppm), 3.3 broad (CH—S, 6H), 2.3 s (CH₃—CO—, 18H), 1.1–2.0 broad (—CH₂— and —CH—, 26H), 0.8–0.9 broad (CH₃—, 24H). FTIR (ATR, cm⁻¹): 2960, 2925, 1680, 1450, 1380, 1365, 1110, 1140, 950, 752, 620.

Hydrolysis of 6STA-SQ (6SH-SQ). 6STA-SQ (9 g, 10.4 mmol) was put in a round-bottomed flask with 60 mL of methanol and 1.8 g (45 mmol) of pulverized NaOH and vigorously stirred for 5.5 h at reflux temperature and in inert atmosphere. The solution was allowed to cool and the solvent was removed. The product obtained was dissolved in water and acidified with 0.1 mol L⁻¹ HCl solution and then extracted with CHCl₃. The organic phase was washed with distilled water and dried over anhydrous MgSO₄. After solvent evaporation the purification of 6SH-SQ was carried out by silica gel column chromatography using hexane/ethyl acetate (8/2) mixture as eluent. The purified product was a pale yellow viscous liquid in 71% yield. ¹H NMR (CDCl₃; δ , ppm), 2.60 broad (—CH—S—, 6H), 1.10–1.95 unresolved broad signals (—CH₂—, —CH— and —SH, 32H), 0.8–1.05 broad (CH₃—, 24H). FTIR (ATR, cm⁻¹): 2955, 2923, 2570, 1450, 1378, 1350, 752. Spectra are fully coincident with those reported in the literature.²²

Synthesis of thiol from triallyl isocyanurate (3SH-ISO)

Photochemical thiol-ene reaction (3STA-ISO). A mixture of 6 g (24.1 mmol) of TAIC and 21.98 g (288.7 mmol) of TAA was photoirradiated with a UV lamp at 356 nm for 1 h adding 0.1286 g (0.5 mmol) of DMPA as photoinitiator. The product was dissolved in CHCl₃ and extracted with a saturated NaOH solution and then washed with water and dried over anhydrous MgSO₄. The solvent was removed using a rotary evaporator and the product obtained was a white solid in 96% yield (m.p. 77 °C). ¹H NMR (CDCl₃; δ , ppm): 3.90 t (—CH₂—N—, 6H), 2.87 t (—CH₂—S—, 6H), 2.30 s (CH₃—CO—, 9H), 1.90 q (—CH₂—CH₂—CH₂—, 6H). ¹³C NMR (CDCl₃; δ , ppm): 200 (CO—S), 149 (—N—CO—N—), 42 (—N—CH₂—), 30 (CH₃CO—S—), 27 (—CH₂—S—), 25 (—CH₂—CH₂—CH₂—). FTIR (ATR, cm⁻¹): 2800, 2780, 1660, 1458, 1424, 1140, 960, 810, 776, 620.

Hydrolysis of 3STA-ISO (3SH-ISO). STA-ISO (11.92 g, 25 mmol) was put into a round-bottomed flask equipped with a magnetic stirrer with 120 mL of methanol and 2.15 g (53.8 mmol) of pulverized NaOH. The solution was maintained for 5.5 h at reflux temperature under inert atmosphere and then allowed to cool and the solvent was removed. The solid obtained was dissolved in water and acidified with 0.1 mol L⁻¹ HCl solution. Then, it was extracted with CHCl₃ and the organic phase was washed with distilled water several times and dried over anhydrous MgSO₄. The thiol 3SH-ISO obtained after the solvent evaporation was a colourless viscous liquid, 95% yield. ¹H NMR (CDCl₃; δ , ppm): 4.05 t (—CH₂—N—, 6H), 2.60 (—CH₂—S, 6H), 1.95 q (—CH₂—CH₂—CH₂—, 6H), 1.60 t (—SH, 3H). ¹³C NMR (CDCl₃; δ , ppm): 149.5 (—N—CO—N—), 42.0 (CH₂—N), 32.5 (CH₂—SH) and 21 (—CH₂—CH₂—CH₂—). FTIR (ATR, cm⁻¹): 2800, 2778, 2570, 1675, 1456, 1420, 772.

Synthesis of thiol from eugenol (3SH-EU)

The trithiol of EU was prepared from EU using a five-step synthetic procedure.

Preparation of triallyl eugenol (3A-EU). Triallyl eugenol was prepared following a previously reported procedure.²³

Synthesis of 1-allyl-4-allyloxy-3-methoxybenzene (2A-EU). Eugenol (16.4 g, 100 mmol) and 4.40 g of pulverized NaOH (110 mmol) were dissolved in 120 mL of dry DMF in a 500 mL three-necked round-bottomed flask under inert atmosphere. The mixture was stirred for 10 min and then allyl bromide (13.30 g, 110 mmol) was added dropwise over 1 h at 40 °C. Once the addition was finished the solution was maintained at 40 °C for 3 h and then 0.5 h at 70 °C. The solvent was eliminated in a rotavap and the oil was dissolved in CHCl₃ and filtered to eliminate the precipitate of inorganic salts. The organic phase was washed twice with distilled water, dried over anhydrous MgSO₄ and the solvent eliminated to obtain 96% yield of 2A-EU as a yellowish oil. ¹H NMR (CDCl₃; δ , ppm): 6.7 d (Ar, 1H), 6.6 m (Ar, 2H), 6.1 m (—CH=, 1H), 5.9 m (—CH=, 1H), 5.3 dd (CH₂=, 1H), 5.2 dd (CH₂=, 1H), 5.0 m (CH₂=, 2H), 4.50 d (—CH₂—O—, 2H), 3.8 s (CH₃—O—, 3H), 3.3 d (—CH₂—Ar, 2H). ¹³C NMR (CDCl₃; δ , ppm): 149.2 (Ar), 146.2 (Ar), 137.8 (—CH=CH₂), 133.7 (—CH=CH₂), 133.0 (Ar), 120.2 (Ar), 118.0 (=CH₂), 115.8 (=CH₂), 113.5 (Ar), 112.0 (Ar), 70.0 (—CH₂—O—), 56.0 (CH₃—O—), 40.0 (—CH₂—). FTIR (ATR, cm⁻¹): 3070, 3015, 2970, 2830, 1680, 1630, 1592, 1505, 1460, 1423, 1250, 1225, 1145, 1023, 997, 910, 850, 803, 749.

Pyrolysis of 1-allyl-4-allyloxy-3-methoxybenzene (r2A-EU). In a glass tube provided with a gas outlet 19.48 g (95.5 mmol) of 2A-EU was stirred at 200 °C for 3 h to obtain a 98% yield of a yellowish oil. ¹H NMR (CDCl₃; δ , ppm): 6.59 s (Ar, 2H), 5.91 m (—CH=, 2H), 5.6 s (—OH, 1H), 5.1 m (CH₂=, 4H), 3.9 s (CH₃—O—, 3H), 3.4 dd (—CH₂—Ar, 2H) and 3.3 dd (—CH₂—Ar, 2H). ¹³C NMR (CDCl₃; δ , ppm): 146.4 (Ar), 141.6 (Ar), 138.0 (—CH=CH₂) 136.8 (—CH=CH₂), 131.1 (Ar), 125.5 (Ar), 122.0 (Ar), 115.5 (=CH₂), 115.4 (=CH₂), 108.9 (Ar), 56.0 (CH₃—O—), 40.0 (—CH₂—), 34.0 (—CH₂—). FTIR (ATR, cm⁻¹): 3540, 3075, 3012, 2970, 2900, 2845, 1630, 1605, 1442, 1498, 1293, 1227, 1205, 1146, 1070, 993, 910, 848, 750.

Synthesis of 1,3-diallyl-4-allyloxy-5-methoxybenzene (3A-EU). The previously obtained r2A-EU (19.14 g, 94 mmol), 4.13 g (103 mmol) of pulverized NaOH and 120 mL of DMF were placed in a three-necked round-bottomed flask under inert atmosphere. The mixture was stirred for 10 min and then allyl bromide (12.49 g, 105 mmol) was added dropwise over 1 h at 40 °C. Once the addition was completed the mixture was kept at 40 °C for 3 h and then 0.5 h at 70 °C. The reaction product was treated with distilled water to dissolve the NaBr formed and extracted with chloroform. The

organic phase was washed twice with distilled water, dried with anhydrous MgSO₄ and concentrated using a rotary evaporator to obtain 97% yield of 3A-EU as a yellowish oil. ¹H NMR (CDCl₃; δ, ppm): 6.7 s (Ar, 2H), 6.05 m (—CH=, 1H), 5.90 m (—CH=, 2H), 5.34 dd (CH₂=, 1H), 5.19 dd (CH₂=, 1H), 5.15—5.0 m (CH₂=, 4H), 4.46 d (—CH₂—O—, 2H), 3.87 s (CH₃—O—, 3H), 3.38 d (—CH₂—Ar, 2H), 3.31 d (—CH₂—Ar, 2H). ¹³C NMR (CDCl₃; δ, ppm): 152.6 (Ar), 144.1 (Ar), 137.5 (—CH=CH₂), 137.3 (—CH=CH₂), 135.7 (Ar), 134.5 (Ar), 133.7 (—CH=CH₂), 121.7 (Ar), 117.0 (=CH₂), 115.8 (=CH₂), 115.5 (=CH₂), 110.5 (Ar), 73.7 (—CH₂—O—), 55.7 (CH₃—O—), 40.1 (—CH₂—), 34.3 (—CH₂—). FTIR (ATR, cm⁻¹): 3072, 3018, 2901, 2825, 1637, 1583, 1510, 1451, 1418, 1256, 1230, 1141, 1026, 986, 907, 804, 752.

Photochemical thiol-ene reaction (3STA-EU). A mixture of 5 g (20.5 mmol) of triallyl eugenol derivative (3A-EU), 22.2 g (291.6 mmol) of TAA and 0.1290 g (0.50 mmol) of DMPA were photoirradiated with a UV lamp at 356 nm for 1 h. The product obtained was dissolved in CHCl₃ and extracted with a saturated NaOH solution and then washed with water and dried over anhydrous MgSO₄. The solvent was removed using a rotary evaporator. The product obtained was a viscous liquid in 96% yield. ¹H NMR (CDCl₃; δ, ppm): 6.52 s and 6.50 s (Ar, 2H), 3.91 t (—CH₂—O—, 2H), 3.80 s (CH₃—O—, 3H), 3.10 (—CH₂—S—, 2H), 2.85 m (—CH₂—Ar, 4H), 2.56 m (—CH₂—S—, 4H), 2.31 s (CH₃—CO—S—, 9H), 1.99 m (—CH₂—CH₂—CH₂—O—, 2H), 1.8 m (—CH₂—CH₂—CH₂—Ar, 4H). ¹³C NMR (CDCl₃; δ, ppm): 195.7, 195.6 and 195.5 (3C, —CO—S—), 152.3 (Ar), 143.9 (Ar), 136.6 (Ar), 134.5 (Ar), 121.4 (Ar), 110.3 (Ar), 70.0 (—O—CH₂—), 55.5 (CH₃—O—), 34.5 and 31.0 (—CH₂—Ar), 30.5, 30.3 and 30.2 (3C, CH₃CO—S—), 29.1, 28.7 and 28.4 (3C, CH₂—S—), 25.8 (3C, CH₂—CH₂—CH₂—). FTIR (ATR, cm⁻¹): 2930, 2825, 1680, 1587, 1505, 1460, 1424, 1355, 1260, 1232, 1135, 1010, 950, 800, 607.

Hydrolysis of 3STA-EU (3SH-EU). 3STA-EU (9.31 g, 19.7 mmol) was added to 100 mL of methanol in a flask equipped with magnetic stirrer. An amount of 1.70 g (42.5 mmol) of pulverized NaOH was added and the mixture heated at reflux temperature under inert atmosphere for 5.5 h. The solution was allowed to cool and the solvent was removed. The product obtained was dissolved in water and acidified with 0.1 mol L⁻¹ HCl solution and then extracted with CHCl₃. The organic phase was washed with distilled water and then dried over anhydrous MgSO₄. The product obtained was a pale yellow viscous liquid in 84% yield. ¹H NMR (CDCl₃; δ, ppm): 6.56 s (Ar, 2H), 3.98 t (—CH₂—O—, 2H), 3.82 s (CH₃—O—, 3H), 2.77 q (—CH₂—S—, 2H), 2.61 m (—CH₂—S—, 4H), 2.51 q (—CH₂—Ar, 4H), 2.1 m (—CH₂—CH₂—CH₂—O—, 2H), 1.85 m (—CH₂—CH₂—CH₂—Ar, 4H), 1.5 t (—SH, 1H), 1.35 t (—SH, 1H), 1.33 t (—SH, 1H). ¹³C NMR (CDCl₃; δ, ppm): 152.2 (Ar), 143.9 (Ar), 136.7 (Ar), 134.6 (Ar), 121.5 (Ar), 110.2 (Ar), 70.3 (—O—CH₂—), 55.5 (CH₃—O—), 35.3 (—CH₂—Ar), 34.6, 34.3 and 34.0 (3C, —CH₂—SH), 28.5 (—CH₂—Ar), 24.1, 23.8 and 21.2 (3C, CH₂—CH₂—CH₂—). FTIR (ATR, cm⁻¹): 2930, 2825, 2580, 1587, 1503, 1460, 1430, 1260, 1230, 1150, 1090, 1010, 950, 830.

Preparation of curing mixtures and samples

The mixtures were prepared by mixing stoichiometric amounts of epoxide/SH groups (1:1) of ECC with the various thiols. It should be taken into account that the functionality of ECC is 2 and the functionalities of the thiols are 6 for SQ-6H, 4 for PETMP and 3 for both 3SH-ISO and 3SH-EU in this reactive process. In catalysed formulations, 2 phr of basic catalyst (parts of catalyst per hundred parts of epoxy resin) was added after homogenization of ECC/thiol mixture with a spatula. Formulations were prepared using four

different catalysts in order to test their activity and choose the most suitable one for the thermal curing process.

Characterization techniques

¹H NMR and ¹³C NMR spectra were recorded with a Varian Gemini 400 spectrometer. CDCl₃ was used as the solvent. For internal calibration the solvent signal corresponding to CDCl₃ was used: δ (¹H) = 7.26 ppm, δ (¹³C) = 77.16 ppm.

A Jasco Fourier transform infrared (FTIR) spectrometer (resolution of 4 cm⁻¹) with an attenuated total reflectance (ATR) accessory with a diamond crystal (Golden Gate heated single-reflection diamond ATR, Specac-Teknokroma). All the measurements were performed at room temperature. FTIR spectra were used to follow the formation of thiol band at 2570 cm⁻¹ and the evolution of the curing process of the different formulations. In this case, the spectra were collected before and after thermal process.

A DSC instrument (Mettler DSC-821e) calibrated using an indium standard (heat flow calibration) and an indium–lead–zinc standard (temperature calibration) was used to determine the evolution and kinetics of the curing process. Samples of ca 10 mg were analysed under non-isothermal conditions under a constant nitrogen atmosphere with a gas flow of 100 mL min⁻¹. The non-isothermal studies were performed in the temperature range 30 to 240 °C, with heating rates of 2, 5, 10 and 15 °C min⁻¹.

Values of T_g of the final thermosets were determined after two consecutive dynamic heating scans at 20 °C min⁻¹ starting at -20 °C with a Mettler DSC-822e device to delete the thermal history. The T_g value was taken as the middle point in the heat capacity step of the glass transition.

The degree of conversion by DSC was calculated as follows:

$$\alpha = \frac{\Delta h_T}{\Delta h_{dyn}} \quad (1)$$

where Δh_T is the heat released up to a temperature T or up to a time t, obtained by integration of the calorimetric signal up to this temperature or time, and Δh_{dyn} is the total reaction heat associated with the complete conversion of all reactive groups.

The linear integral isoconversional, model-free method of Kissinger–Akahira–Sunose was used for the determination of the activation energy based on the non-isothermal curing curves:²⁴

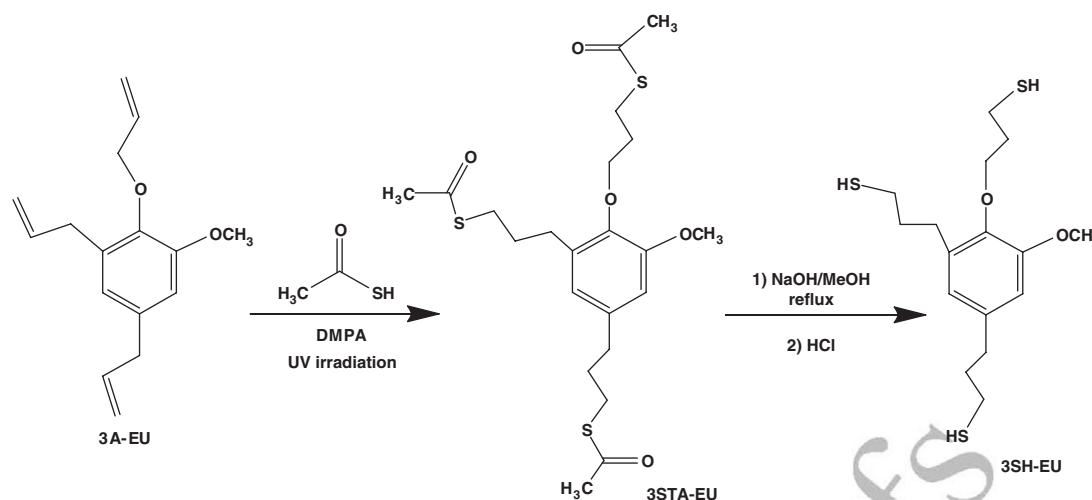
$$\ln \left(\frac{\beta}{T^2} \right) = \ln \left(\frac{AR}{g(\alpha)E} \right) - \frac{E}{RT} \quad (2)$$

where β is the heating rate, T the temperature, E the activation energy, A the pre-exponential factor, R the gas constant and g(α) the integral conversion function. For each degree of conversion, a representation of ln(β/T²) versus 1/T produces a straight line and makes it possible to determine E and ln[AR/g(α)E] from the slope and the intercept without knowing the kinetic model.

Assuming that the approximation given by Eqn (2) is valid, we can determine the kinetic model that best describes the curing process by rearranging Eqn (2) as

$$\ln \left(\frac{g(\alpha)\beta}{T^2} \right) = \ln \left(\frac{AR}{E} \right) - \frac{E}{RT} \quad (3)$$

which is the basis for the composite integral method for the determination of the kinetic model.²⁵ A plot of ln(g(α)β/T²) against -1/RT for all heating rates should yield a perfectly straight line, with a slope E equivalent to the isoconversional activation energy



Scheme 2. Two-step synthetic procedure for the transformation of triallyl eugenol (3A-EU) to the trithiol of eugenol (3SH-EU).

if the kinetic model $g(\alpha)$ is applicable. Given that the curing of epoxy–thiol reactions can be satisfactorily modelled using autocatalytic kinetic models,^{6,26} we have fitted the experimental data to autocatalytic kinetic models with $n + m = 2$, where n and m are the non-catalytic and catalytic orders of reaction, respectively. Details of the model fitting methodology used can be found elsewhere.²⁷

The thermal stability of cured samples was evaluated using TGA, with a Mettler TGA/SDTA 851e thermobalance. All experiments were performed under inert atmosphere (nitrogen at 100 mL min⁻¹). Pieces of the cured samples with an approximate mass of 8 mg were degraded between 30 and 600 °C at a heating rate of 10 K min⁻¹.

Dynamic mechanical thermal analysis (DMTA) was carried out with a TA Instruments DMA Q800 analyser. The samples were prepared as described before. Three-point bending clamp was used on prismatic rectangular samples (15 mm × 7.9 mm × 1.5 mm). The curing schedule applied to cure the samples was 1 h at 120 °C, 1 h at 150 °C and a final post-curing at 200 °C for 30 min. Samples were first heated at 5 K min⁻¹ from 30 to 180 °C to erase the thermal history and then analysed at 3 K min⁻¹ from 30 to 180 °C at a frequency of 1 Hz with an oscillation amplitude of 10 μm. Young's modulus was determined by a stress/strain test, under the same clamp and geometry testing conditions, at 30 °C using a force ramp of 3 N min⁻¹ and upper force limit of 18 N.

RESULTS AND DISCUSSION

Synthesis of thiols from vinylic compounds

The synthesis of the various thiols was carried out following a two-step procedure starting from the vinyl compounds as reported for squalene derivatives.²² The first synthetic step consists of a photochemical thiol–ene click reaction of TAA to the multifunctional ene compound in the presence of a radical photoinitiator. The thiol–ene reaction is not inhibited by oxygen, which constitutes a great advantage in technological applications. The radical formed by the photocleavage of the photoinitiator abstracts a hydrogen atom from TAA, generating a thiyl radical that is added to a reactive double bond of the vinyl compound creating a carbon radical. The carbon radical abstracts a hydrogen from a thiol group, generating a new thiyl radical.⁵ This alternating mechanism, cycling between thiyl addition to the double bond

and chain transfer leading to a new thiyl radical, results in the consumption of thiol and ene groups at the same rate. If stoichiometric thiol–ene mixtures are used, complete reaction of thiol and ene groups is achieved. The second step in the thiol synthesis is the hydrolysis reaction of the corresponding thioacetate by treatment with a methanolic solution of NaOH at reflux temperature, followed by acidification with diluted HCl. This synthetic procedure, previously described for the preparation of the thiol derived from squalene (6SH-SQ),²² has been successfully applied in the present study for the synthesis of 3SH-EU and 3SH-ISO from the corresponding triallyl derivatives, the yields being notably high. The two-step synthetic process is represented for the eugenol derivative in Scheme 2.

Structural characterization of synthesized thiols and their synthetic intermediates

The FTIR characterization of the products prepared renders as the most typical absorptions a strong band at 1700 cm⁻¹ of carbonyl stretching for the intermediate thioacetates and a weak band at 2560 cm⁻¹, assigned to the SH absorption for all the thiols prepared. The structure of the products prepared was confirmed using ¹H NMR spectroscopy.

The ¹H NMR spectra of squalene derivatives were compared to those previously published, showing complete agreement.²² The complex structure that includes a great number of stereoisomers makes the structural characterization using this technique difficult but the appearance of acetate peaks in the spectra of intermediate materials and the complete elimination by saponification are valuable indicators to confirm that the synthetic process has occurred as expected.

The trithiol derived from triallyl isocyanurate (3SH-ISO) has not been reported in the literature up to now. The structure of this compound and that of the intermediate thioacetate were determined from their ¹H NMR spectra, which are shown in Fig. 1. The spectra present few signals according to the third-order symmetry axis.

In the spectrum of 3STA-ISO the most characteristic signal is the peak at 2.31 ppm corresponding to the methyl protons of the thioacetate group that appears as a singlet, which has disappeared completely in the spectrum of 3SH-ISO. It is worth noting that signals corresponding to vinyl protons cannot be observed in the spectrum of 3STA-ISO, which confirms that the photoinduced

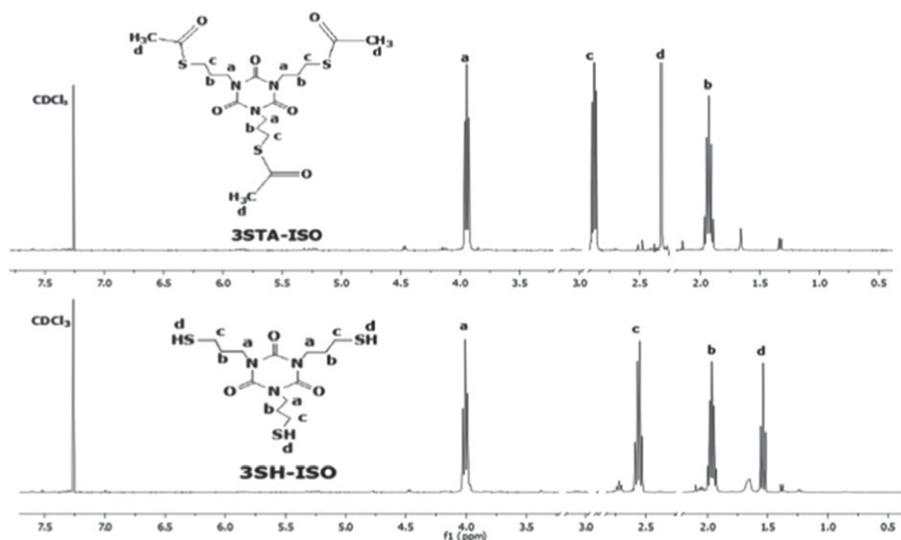


Figure 1. ^1H NMR spectra of trithioacetate (3STA-ISO) and trithiol (3SH-ISO) derived from triallyl isocyanurate recorded in CDCl_3 .

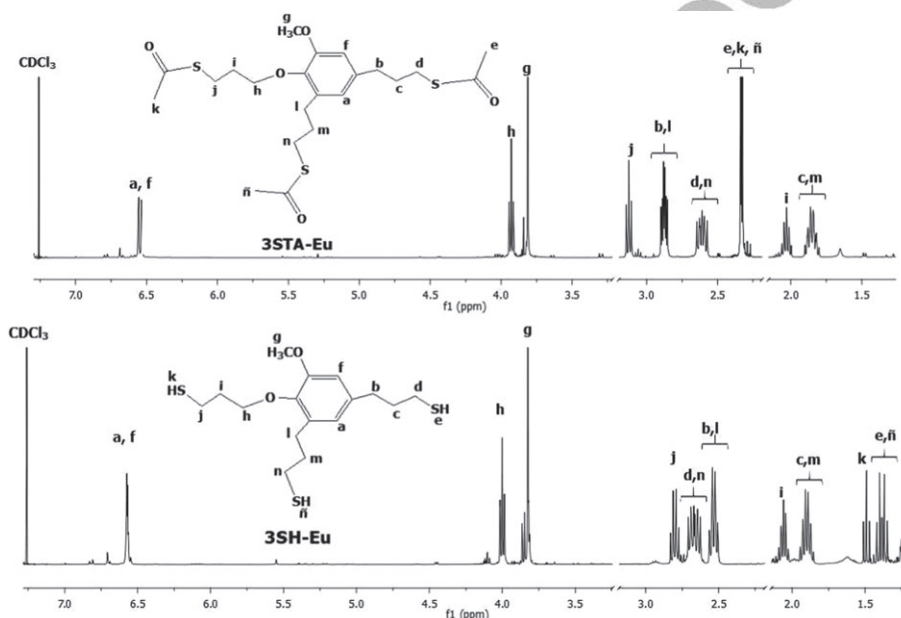


Figure 2. ^1H NMR spectra of trithioacetate (3STA-EU) and trithiol (3SH-EU) derived from eugenol recorded in CDCl_3 .

thioacetic addition to triallyl isocyanurate was complete. Signals *a* and *b* at about 3.95 and 1.9 ppm practically remain unchanged in both spectra. However, the signal corresponding to the methylene protons *c*, which appears as a triplet at 2.87 ppm in the acetate spectrum shifts to 2.55 ppm after hydrolysis and shows a more split peak because of the coupling with the proton of the thiol that appears as a triplet at 1.55 ppm in the thiol spectrum. The ^{13}C NMR spectrum of 3SH-ISO is shown in Fig. A in the supporting information.

Figure 2 shows the spectra of the eugenol derivatives. As in the previous case, the thiol-ene process is complete since no vinylic protons appear in the 3STA-EU spectrum. As before, the formation of the thiol is confirmed by the disappearance of the peak at 2.34 ppm, corresponding to the methyl protons from the thioacetate groups. However, the eugenol derivative has no symmetry and therefore more signals appear, making the assignment more difficult.

In a similar way to what happens in the TAIC derivatives, the presence of thiol leads to a higher splitting of the methylene protons attached to this group. The three signals due to the thiol protons appear as triplets below 1.5 ppm, two of them partially overlapped by the similarity of the electronic surroundings.

The ^{13}C NMR spectrum was also recorded and it is shown in Fig. B in the supporting information.

Study of curing process

The reaction of thiolates with epoxides follows a nucleophilic $\text{S}_{\text{N}}2$ mechanism with well-defined stereochemical control. Thiols require an amine as basic catalyst to increase their nucleophilic character by the formation of thiolates.^{6,7,20} However, the use of bases like trimethylamine in thiol-DGEBA reactions leads to too short a pot-life that makes application difficult.²⁸ For that reason the use of a latent basic catalyst is recommended.⁷

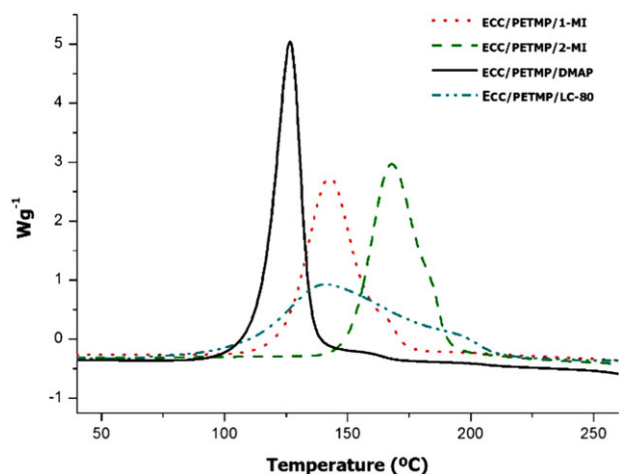


Figure 3. DSC thermograms corresponding to dynamic curing at $10\text{ }^{\circ}\text{C min}^{-1}$ of cycloaliphatic resin/PETMP mixtures with a proportion of 2 phr of the various catalysts.

With the aim of selecting the best basic catalyst to perform the thermal curing of ECC, different amines, 1-MI, 2-MI, DMAP and LC-80, were tested. All of them are tertiary amines, LC-80 being an encapsulated imidazole. The DSC thermograms corresponding to thermal curing of ECC/PETMP stoichiometric formulations with 2 phr of each catalyst are shown in Fig. 3.

It can be observed in Fig. 3 that the formulation catalysed by LC-80 begins to cure at relatively low temperature and finishes at about $200\text{ }^{\circ}\text{C}$ showing a low curing rate and a broad curing temperature range. On the other hand, the curing with DMAP starts around $100\text{ }^{\circ}\text{C}$, with a very fast curing reaction that finishes at about $140\text{ }^{\circ}\text{C}$ in a narrow temperature range. 1-MI shows an intermediate activity and 2-MI is the one that is activated at the highest temperature.

In previous studies of the curing of DGEBA resins with thiols we used 2 phr of LC-80 as the catalyst and its latent character was demonstrated.⁷ However, according to our experience, various catalysts can be used and the most appropriate depends on the composition of the formulation.²⁹ We also reported^{7,30} that the curing of mixtures of DGEBA and PETMP or trimethylolpropane tris(3-mercaptopropionate) (TTMP) with smaller amounts of catalysts such as 1-MI and LC-80 took place at lower temperatures. It is well known that primary amines are not able to cure cycloaliphatic epoxy resins,³¹ so it could be expected that the curing of ECC with thiol crosslinkers would be more difficult but, as seen in Fig. 3, it takes place within an acceptable temperature range. Given that the curing with DMAP is activated within the same temperature range as the curing with latent catalyst LC-80, and that the curing takes place within a narrower temperature range, it is suggested that DMAP is the most suitable catalyst for these systems.

The effect of the various catalysts was also analysed for the different formulations prepared from the synthesized thiol crosslinkers. Figure 4 shows, as an example, that the activity of the various catalysts in formulations using 6SH-SQ as thiol crosslinking agent follows the same trend as with PETMP. In the case of 3SH-ISO and 3SH-EU (Figs C and D in the supporting information), similar results are obtained and DMAP is the most active catalyst, with an activation temperature close to that of LC-80. Therefore, DMAP was selected as the most suitable catalyst and used for further studies in this work.

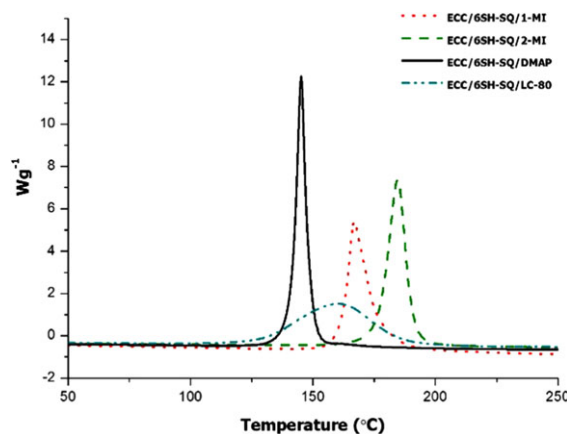


Figure 4. DSC thermograms corresponding to dynamic curing at $10\text{ }^{\circ}\text{C min}^{-1}$ of ECC/6SH-SQ stoichiometric mixtures with 2 phr of the various catalysts.

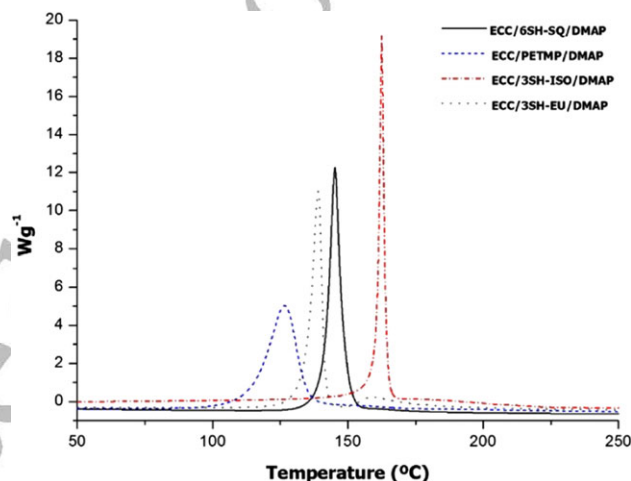


Figure 5. DSC thermograms corresponding to dynamic curing at $10\text{ }^{\circ}\text{C min}^{-1}$ of mixtures of cycloaliphatic resin with different thiols using DMAP as catalyst.

Figure 5 collects the calorimetric curves for the curing of ECC with the four thiols selected using 2 phr of DMAP as the catalyst. It is known³² that the structure and the chemical environment of the thiol group have a very strong influence on its pK_a and the nucleophilicity of the thiolate anion. Thus, it could be expected that 6SH-SQ would be less reactive than PETMP due to the lower nucleophilicity of the thiolate anion. It can be seen that the less reactive thiol crosslinker, with highest activation temperature, is the one derived from triallyl isocyanurate.

Table 1 summarizes the values of enthalpy released and the temperatures of the maximum of the calorimetric peaks for the curing of the mixtures with various thiols and DMAP as the catalyst. As we can see, the heat released by epoxy equivalent is higher than 100 kJ eq^{-1} for all the mixtures with the synthesized thiols and a little higher for the commercial PETMP. In DGEBA/PETMP formulations catalysed by LC-80 enthalpies of 127 kJ eq^{-1} were measured during curing. The curing of ECC with PETMP releases a comparable amount of heat, but the other thiol crosslinkers lead to lower enthalpy released per epoxy equivalent. On the one hand, there are experimental uncertainties associated with the baseline determination and integration of the curing peaks, especially those

Table 1. Calorimetric data and kinetic parameters obtained for curing of formulations with various thiols containing 2 phr of DMAP

Formulation	Δh^a (J g ⁻¹)	Δh^a (kJ eq ⁻¹)	T_{max} (°C)	E_a^b (kJ mol ⁻¹)	$\ln A^c$ (min ⁻¹)	$k_{130^\circ C}^c$ (min ⁻¹)	$(d\alpha/dt)_{0.5}^d$ (min ⁻¹)
ECC/6SH-SQ	473.1	108.1	145	65.8	20.3	1.98	0.50
ECC/PETMP	511.8	131.0	127	61.0	19.1	2.45	0.61
ECC/3SH-ISO	435.9	107.0	163	65.9	20.0	1.39	0.35
ECC/3SH-EU	430.2	107.7	134	68.6	21.2	2.15	0.54

^a Curing enthalpy measured in a DSC scan at 10 °C min⁻¹.
^b Kinetic parameters obtained by model-fitting using an autocatalytic model with $n + m = 2$.
^c Values of rate constant at 130 °C using the Arrhenius equation and the parameters E and $\ln A$.
^d Values of reaction rate at 130 °C obtained using the rate equation $d\alpha/dt = kf(\alpha) = k(1 - \alpha)^n \alpha^m$ at 50% conversion.

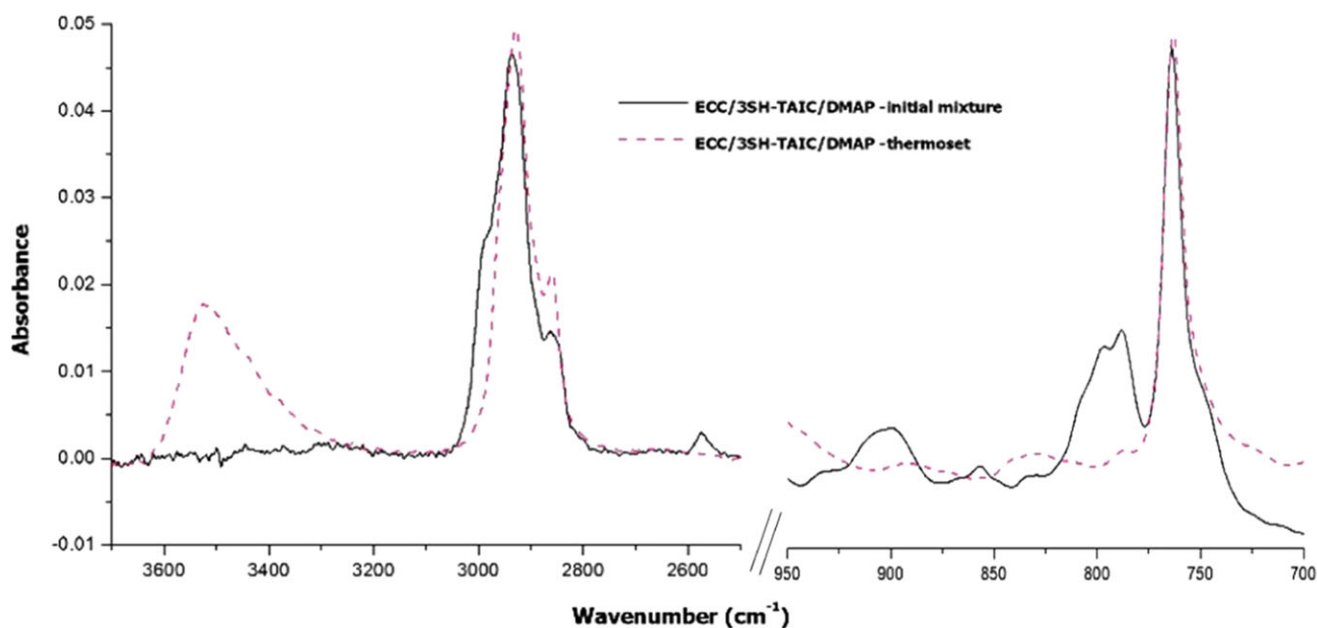


Figure 6. FTIR spectra of mixture ECC/3SH-ISO catalysed by 2 phr of DMAP before and after curing.

extending to higher temperatures, where side degradation reactions might also occur. On the other hand, it may be hypothesized that PETMP leads to somewhat higher conversion than the other thiols, due to its more flexible structure. For instance, one could expect some topological hindrance leading to incomplete cure for 6SH-SQ, because of its small molecular size and high functionality. It might be argued likewise in the case of 3SH-ISO and 3SH-EU, with a rigid core structure and flexible but short arms.

However, FTIR-ATR analysis of the cured samples shows that the curing is quantitative. Figure 6 shows, as an example, the most significant regions of the spectra before and after curing of the formulation cured with 3SH-ISO. The initial spectrum shows the typical absorptions of S—H stretch at 2570 cm⁻¹ and the band at 795 cm⁻¹ corresponding to the cycloaliphatic epoxy ring. Both bands have disappeared completely in the spectrum of the cured material, confirming that the curing is complete. In addition, a new broad absorption at 3500 cm⁻¹ appears because of the formation of the β -hydroxythioether group in the network structure.

The kinetics of the curing of the various formulations was studied using DSC. From calorimetric curves obtained at different heating rates and applying the isoconversional methodology we could determine the activation energy of these curing processes. Figure 7 shows the evolution of activation energy during the curing process. No great differences among them are observed and

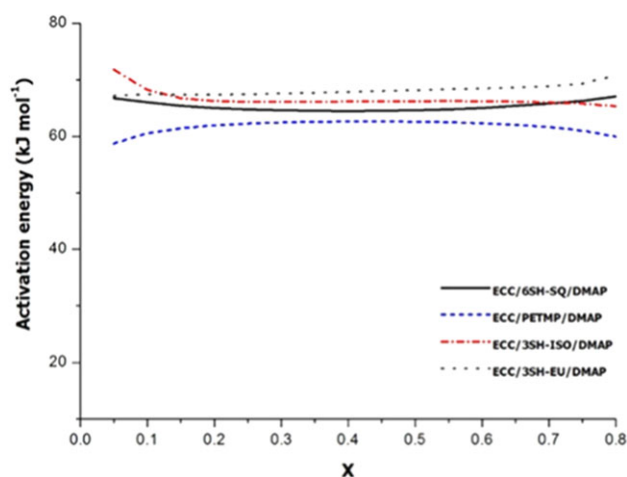


Figure 7. Activation energy versus degree of conversion of cycloaliphatic resin with various thiols using DMAP as catalyst.

the values are more or less constant during all the curing process indicating that the reaction mechanism is the same during the whole curing time and no epoxy homopolymerization occurs, as expected for stoichiometric thiol–epoxy formulations.^{30,33} The



Figure 8. Photographs of thermosets obtained from various ECC/thiol formulations catalysed by 2 phr of DMAP: (A) 6SH-SQ; (B) PETMP; (C) 3SH-ISO; (D) 3SH-EU.

Formulation	DSC		TGA		DMTA	
	T_g^a (°C)	$T_{5\%}^b$ (°C)	T_{max}^c (°C)	$T_{tan\delta}^d$ (°C)	Young's modulus ^e (MPa)	E_r^f (MPa)
ECC/6SH-SQ	116	322	341	135	2231	15.8
ECC/PETMP	53	268	336	80	2048	8.0
ECC/3SH-ISO	70	327	377	91	2070	7.6
ECC/3SH-EU	69	294	367	88	2043	6.8

^a Glass transition temperature determined by DSC at 10 °C min⁻¹ from -20 to 250 °C.
^b Temperature of 5% of weight loss in nitrogen atmosphere.
^c Temperature of maximum rate of degradation in nitrogen atmosphere.
^d Temperature of maximum of tan δ determined by DMTA.
^e At 30 °C.
^f Storage modulus in the rubbery state at $T = T_{tan\delta} + 50$ °C.

apparent activation energy during curing of thiol-epoxy formulations depends largely on the type and proportion of catalyst⁷ and in consequence on the underlying curing mechanism.^{26,30,33} Therefore, comparison with other systems is difficult, but the values are in general agreement with those of previous reports.^{7,30}

Given that the isoconversional activation energy is constant, it is possible to model the curing kinetics using a kinetic model with a single rate constant. Given that the curing kinetics of thiol-epoxy formulations with tertiary amines has an autocatalytic behaviour,^{26,30,33} we selected an autocatalytic kinetic model of type $n + m = 2$ to fit our experimental results. The kinetic values of the curing of the formulations with various thiols are collected in Table 1. The kinetic constant and reaction rate at 130 °C of the curing process are significantly affected by the reactivity of the thiol employed. The results obtained show that PETMP is the most reactive, followed by 3SH-EU and 6SH-SQ. The least reactive thiol is 3SH-ISO which needs higher temperature to be initiated. These results agree with the trend in reactivity shown in Fig. 5.

Characterization of thermosets

The thermosets obtained by curing the four formulations with the various thiols were thermally characterized using DSC, TGA and DMTA. The formulations were cured with the following schedule: 1 h at 120 °C, 1 h at 150 °C and a post-curing of 0.5 h at 200 °C. The materials obtained are transparent as previously reported for thiol-epoxy materials⁷ and the colour depends on the thiol used in the curing. Figure 8 shows the corresponding photographs.

Table 2 collects the main data obtained from the thermal characterization. T_g determined using DSC is correlated with the structural characteristics of the thiol. PETMP, with a functionality of 4 but

quite a flexible structure, leads to T_g of 53 °C. In spite of the different epoxy used, this value compares well with that obtained for DGEBA/PETMP materials.²⁰ Trifunctional thiol crosslinkers with a rigid core, 3SH-ISO and 3SH-EU, lead to materials with comparable T_g of 69 and 70 °C, which are significantly higher than those that can be obtained using a flexible trifunctional crosslinker such as TTMP.⁷ The squalene derivative, 6SH-SQ, with an aliphatic structure but higher functionality, leads to a material with the highest T_g of 116 °C. This can be explained by the densely crosslinked structure, with internal branching points in the thiol crosslinker structure and very short distance between crosslinks.

Figure 9 plots the loss factor tan δ against temperature for the four thermosets prepared, determined using DMTA. The tan δ peak temperature shows the same trend as T_g measured using DSC (Table 2), but the values are higher due to the effect of the frequency on the α relaxation. The tan δ curves show a narrow unimodal shape, indicating that the materials are homogeneous. The curve corresponding to the thiol 6SH-SQ is the one with the highest tan δ peak temperature and the lowest intensity. This is in agreement with a densely crosslinked network structure, having internal branching points within the structure of the thiol crosslinker with very short arm distance. In contrast, the lowest tan δ peak temperature is obtained with PETMP, given its more flexible structure in spite of its higher functionality, in comparison with 3SH-ISO and 3SH-EU. The differences between the materials obtained with 3SH-ISO and 3SH-EU are not relevant, because of their similar structure.

The evolution of storage moduli measured with DMTA is shown in Fig. 10. The decrease in storage modulus during the mechanical relaxation of the network structure follows the same trend

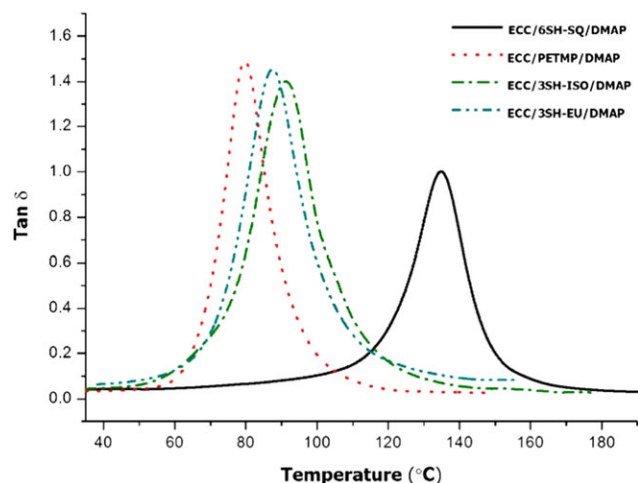


Figure 9. Plots of $\tan \delta$ against temperature for the various materials prepared.

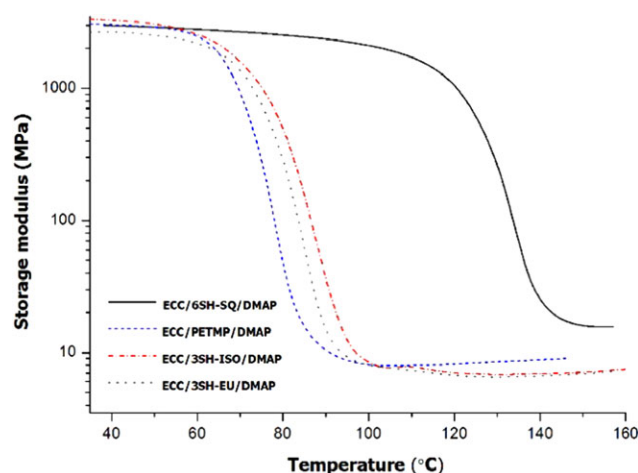


Figure 10. Plot of storage modulus against temperature for the various materials prepared.

as the calorimetric T_g and $\tan \delta$ peak temperature, as expected (Table 2). The material obtained with 6SH-SQ has the highest value of storage modulus in the rubbery state, owing to the higher functionality of the crosslinking agent and the more densely crosslinked network structure.³⁴ Accordingly, PETMP leads to a somewhat higher relaxed modulus than 3SH-ISO and 3SH-EU because of its higher functionality.

The thermal stability of the thermosets was studied using TGA under inert atmosphere. Figure 11 shows the derivative of the degradation curves. As we can see, the degradation of the material with PETMP starts earlier and shows two clear steps, while the others degrade in a single step. The presence of ester groups in PETMP, which are absent in the other thiol crosslinkers, may explain the lower degradation temperature and the multistep degradation process. The most relevant degradation parameters are summarized also in Table 2. The material showing the lowest initial degradation temperature is the thermoset obtained from PETMP because of the existence of a higher proportion of ester groups in the network structure that can degrade much more easily. The highest thermal stability was obtained with 3SH-ISO, because of the presence of the isocyanurate moiety.

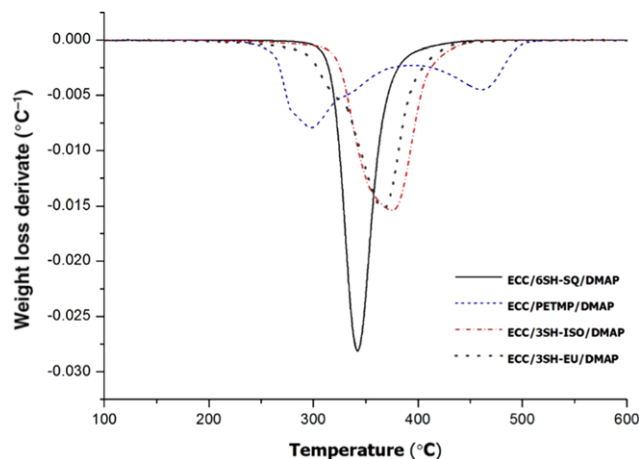


Figure 11. Derivative TGA curves obtained under nitrogen at 10 K min^{-1} of thermosets obtained from ECC and various thiols and 2 phr of DMAP as catalyst.

To summarize, it has been seen that the structure of the thiol crosslinking agent has a very strong influence on the thermomechanical properties of the thermosets prepared from cycloaliphatic epoxy resins, making it possible to meet a wide range of application requirements. In particular, the network structure of thiol-crosslinked ECC thermosets is less densely crosslinked than other ECC thermosets based on epoxy homopolymerization or epoxy-anhydride copolymerization, making it possible to adapt them to less demanding situations from the thermal and mechanical point of view. The greater flexibility of these networks should lead to an improvement in the impact resistance in comparison to homopolymerized cycloaliphatic epoxy thermosets.

CONCLUSIONS

Multifunctional thiols can be easily prepared from vinyl monomers by photochemical thiol-ene reaction with TAA followed by saponification of the acetyl thioesters formed. Using this synthetic method, new trithiols derived from eugenol and triallyl isocyanurate and the hexathiol from squalene were obtained with good yields.

Thermosets based on cycloaliphatic epoxy resin ECC crosslinked with commercially available thiol crosslinker PETMP and other synthesized thiols (6SH-SQ, 3SH-ISO, 3SH-EU) have been prepared using DMAP as catalyst. The reactivity order in the curing process of the thiols tested followed the trend: PETMP > 3SH-EU > 6SH-SQ > 3SH-ISO. Complete reaction of thiol and epoxy groups was confirmed using FTIR spectroscopy.

The obtained materials have lower T_g and storage moduli in the rubbery state than homopolymerized cycloaliphatic epoxy thermosets, derived from ECC, because of their lower crosslinking density and higher flexibility of the network structure, making it possible to adapt ECC thermosets to less demanding applications from the thermal point of view. The structure of the thiol crosslinker had a strong influence on the thermomechanical properties of the resulting materials. The squalene derivative 6SH-SQ led to the highest T_g and moduli in the rubbery state due to its higher functionality and the presence of internal branching points and short arm distances. However, the trithiols derived from eugenol and triallyl isocyanurate present T_g and moduli similar to those of PETMP-derived materials in spite of their different functionality and structure. The synthesized thiol crosslinkers led to



1 more stable thermosets than that obtained with PETMP, because
 2 of the presence of thermally labile ester groups in the latter.

3 4 5 **ACKNOWLEDGEMENTS**

6 The authors thank MINECO (MAT2014-53706-C03-01, MAT2014-
 7 53706-C03-02) and Generalitat de Catalunya (2014-SGR-67 and
 8 Serra Hünter programme) for financial support.

9 10 11 **SUPPORTING INFORMATION**

12 Supporting information may be found in the online version of this
 13 article.

14 15 **REFERENCES**

16 1 Kolb HC, Finn MG and Sharpless KB, *Angew Chem Int Ed* **40**:2004–2021
 17 (2001).
 18 2 Lahann J (ed.), *Click Chemistry for Biotechnology and Materials Science*.
 19 Wiley, Chichester (2009).
 20 3 Moses JE and Moorhouse AD, *Chem Soc Rev* **36**:1249–1262 (2007).
 21 4 Brändle A and Khan A, *Polym Chem* **3**:3224–3227 (2012).
 22 5 Lowe AB and Bowman CN (eds), *Thiol-X Chemistries in Polymer and*
 23 *Materials Science*. RSC Publishing, Cambridge (2013).
 24 6 Meizoso Loureiro R, Carballeira Amarelo T, Paz Abuin S, Soulé ER and
 25 Williams RJJ, *Thermochim Acta* **616**:79–86 (2015).
 26 7 Guzmán D, Ramis X, Fernández-Francos X and Serra A, *Eur Polym J*
 27 **59**:377–386 (2014).
 28 8 Xie M and Wang Z, *Macromol Rapid Commun* **22**:620–623 (2001).
 29 9 Xie M, Wang Z and Zhao Y, *J Polym Sci A: Polym Chem* **39**:2799–2804
 30 (2001).
 31 10 Liu W and Wang Z, *Polym Int* **62**:515–522 (2013).
 32 11 Wang Z, Xie M, Zhao Y, Yu Y and Fang S, *Polymer* **44**:923–929 (2003).
 33 12 Liu W, Wang Z, Xiong L and Zhao L, *Polymer* **51**:4776–4783 (2010).
 34 13 Corcicone CE, Greco A and Maffezzoli A, *J Appl Polym Sci* **92**:3484–3491
 35 (2004).

14 Mas C, Serra A, Mantecón A, Salla JM and Ramis X, *Macromol Chem Phys*
 15 **202**:2554–2564 (2001).
 16 15 Yoo MJ, Kim SH, Park SD, Lee WS, Sun J-W, Choi J-H et al., *Eur Polym J*
 17 **46**:1158–1162 (2010).
 18 16 Belmonte A, Däbritz F, Ramis X, Serra A, Voit B and Fernández-Francos
 19 X, *J Polym Sci B: Polym Phys* **52**:1227–1242 (2014).
 20 17 Fernández X, Salla JM, Serra A, Mantecón A and Ramis X, *J Polym Sci A:*
 21 *Polym Chem* **43**:3421–3432 (2005).
 22 18 Carioscia JA, Stansbury JW and Bowman CN, *Polymer* **48**:1526–1532
 23 (2007).
 24 19 Nair DP, Cramer NB, Gaipa JC, McBride MK, Matherly EM, McLeod RR
 25 et al., *Adv Funct Mater* **22**:1502–1510 (2012).
 26 20 Guzmán D, Ramis X, Fernández-Francos X and Serra A, *Polymers*
 27 **7**:680–694 (2015).
 28 21 Sangermano M, Vitale A and Dietliker K, *Polymer* **55**:1628–1635 (2014).
 29 22 Acosta Ortiz R, Obregón Blandón EA and Guerrero Santos R, *Green*
 30 *Sustain Chem* **2**:62–70 (2012).
 31 23 Yoshimura T, Shimasaki T, Teramoto N and Shibata M, *Eur Polym J*
 32 **67**:397–408 (2015).
 33 24 Vyazovkin S, Burnham AK, Criado JM, Pérez-Maqueda LA, Popesco C
 34 and Sbirrazzuoli N, *Thermochim Acta* **520**:1–19 (2011).
 35 25 García SJ, Ramis X, Serra A and Suay J, *J Therm Anal Calorim* **89**:233–244
 36 (2007).
 37 26 Jin K, Heath WH and Torkelson JM, *Polymer* **81**:70–78 (2015).
 38 27 Flores M, Fernández-Francos X, Ramis X and Serra A, *Thermochim Acta*
 39 **544**:17–26 (2012).
 40 28 Petrie EM, *Epoxy Adhesive Formulations: Epoxy Curing Agents and Cata-*
 41 *lysts*. McGraw-Hill, New York, pp. 107–109 (2006).
 42 29 Guzmán D, Ramis X, Fernández-Francos X and Serra A, *RSC Adv*
 43 **5**:101623–101633 (2015).
 44 30 Fernández-Francos X, Konuray A-O, Belmonte A, De la Flor S, Serra A
 45 and Ramis X, *Polym Chem* **7**:2280–2290 (2016).
 46 31 May CA (ed.), *Epoxy Resins: Chemistry and Technology*, 2nd edition.
 47 Marcel Dekker, New York (1988).
 48 32 Hoyle CE, Lowe AB and Bowman CN, *Chem Soc Rev* **39**:1355–1387
 49 (2010).
 50 33 Loureiro RM, Amarelo TC, Abuin SP, Soulé ER and Williams RJJ, *Ther-*
 51 *mochim Acta* **616**:79–86 (2015).
 52 34 Lesser AJ and Crawford E, *J Appl Polym Sci* **66**:387–395 (1997).

63
64
65
66
67
68
69
70
71
72
73
74
75
76
77
78
79
80
81
82
83
84
85
86
87
88
89
90
91
92
93
94
95
96
97
98
99
100
101
102
103
104
105
106
107
108
109
110
111
112
113
114
115
116
117
118
119
120
121
122
123
124

Uncorrected Manuscript



(wileyonlinelibrary.com) DOI 10.1002/pi.5336

Research Article

Novel thermosets were prepared by the base-catalysed reaction between a commercial cycloaliphatic resin and various thiol crosslinkers, previously synthesized. This thermal curing process has not been reported up to now.



Novel thermal curing of cycloaliphatic resins by thiol-epoxy

click process with several multifunctional thiols **000**

Dailyn Guzmán, Blai Mateu, Xavier Fernández-Francos, Xavier Ramis and Angels Serra*

Uncorrected Proofs

1
2
3
4
5
6
7
8
9
10
11
12
13
14
15
16
17
18
19
20
21
22
23
24
25
26
27
28
29
30
31
32
33
34
35
36
37
38
39
40
41
42
43
44
45
46
47
48
49
50
51
52
53
54
55
56
57
58
59
60
61
62

63
64
65
66
67
68
69
70
71
72
73
74
75
76
77
78
79
80
81
82
83
84
85
86
87
88
89
90
91
92
93
94
95
96
97
98
99
100
101
102
103
104
105
106
107
108
109
110
111
112
113
114
115
116
117
118
119
120
121
122
123
124



QUERIES TO BE ANSWERED BY AUTHOR

IMPORTANT NOTE: Please mark your corrections and answers to these queries directly onto the proof at the relevant place. DO NOT mark your corrections on this query sheet.

Queries from the Copyeditor:

AQ1. Please confirm that given names (red) and surnames/family names (green) have been identified correctly

AQ2. Figures (3, 4, 5, 6, 7, 8, 9, 10, 11, 12, 13) are supplied with low resolution. Kindly resupply.

